Journal of Power Sources 230 (2013) 44–49

Contents lists available at SciVerse ScienceDirect

Journal of Power Sources

journal homepage: www.elsevier.com/locate/jpowsour

Short communication

Ferrocene as precursor for carbon-coated α-Fe_2O_3 nano-particles for rechargeable lithium batteries

A. Brandt, A. Balducci*

Westfälische Wilhelms-Universität, Institut für Physikalische Chemie/MEET, Corrensstr. 28/30, 48149 Münster, Germany

HIGHLIGHTS

- Ferrocene as precursor of carbon-coated α-Fe_2O_3 nano-particles.
- Precise control of the carbon coating present on the nano-particles.
- Carbon-coated α-Fe_2O_3 nano-particles are easily usable.
- Anodes based on carbon-coated α-Fe_2O_3 nano-particles display excellent performance.

ARTICLE INFO

Article history:
Received 6 July 2012
Received in revised form
20 November 2012
Accepted 29 November 2012
Available online 10 December 2012

Keywords:
Ferrocene
Metallocene
Iron oxide
Carbon coating
Lithium-ion battery

ABSTRACT

Ferrocene can be used as a precursor for the synthesis of carbon-coated α-Fe_2O_3 nano-particles. The pyrolysis of ferrocene leads to the formation of a compound that can be fully converted into carbon-coated α-Fe_2O_3 nano-particles via a simple oxidation in air. This simple, fast and cheap synthetic route enables the realization of carbon-coated nano-particles with particle size in the range of 50–150 nm. Moreover, varying the oxidation temperature, it is possible to control precisely the carbon coating present on the nano-particles. The so obtained carbon-coated α-Fe_2O_3 nano-particles can be easily processed in water to realize composite electrodes with a composition suitable for practical application. When used in combination with conventional electrolytes such electrodes display high specific capacity (over 800 mAh g^{-1} at 0.13 A g^{-1}), excellent cycling retention (higher than 99% after 50 cycles), and remarkable rate performance (over 400 mAh g^{-1} at 5 A g^{-1}).

1. Introduction

The use of nano-materials is nowadays the strategy of choice for the realization of high performance lithium-ion batteries (LIBs) [1]. Nano-materials can guarantee high Li^+ diffusion coefficients, a large contact area between the electrode and the electrolyte, and better rate capability than conventional microscale materials [1,2]. The presence of an effective carbon coating can further improve the performance of these materials in terms of cycling stability and rate capability [3,4]. For these reasons, the synthesis of carbon-coated nano-materials has been intensively studied in the last decades [5].

Among the anodic materials investigated so far, those based on transition metal oxides (MO, M = Cu, Fe, Co, Ni, etc.) attracted considerable attention because of their large specific capacity, which is considerably higher than that of state-of-the-art graphite [6]. MOs belong to the so-called conversion materials, and during electrochemical cycling a complete reduction of MO to metal (M) and lithium oxide (Li_2O) takes place, followed by an oxidation of M to MO [7]. Several MOs have been considered in the past, and among them hematite iron oxide (α-Fe_2O_3) is one of the most studied. The interest for this material is related on the one hand to its high theoretical capacity (1007 mAh g^{-1}), and on the other hand to the fact that α-Fe_2O_3 is one of the safest, environmentally most friendly and less expensive material which can be used in LIBs and, more in general, in energy storage devices [8–16]. So far, however, the introduction of α-Fe_2O_3 as anode in LIBs was hindered by its poor reversibility [15,17]. In the last years several strategies have been proposed to overcome this problem, and the particle size control as well as the use of carbon coating have been shown to be the most effective [4,7,14,18,19]. Also the limiting of the cycling regime to a fraction of the total capacity has been shown to have a positive influence on the α-Fe_2O_3 performance [11]. Nevertheless, all abovementioned strategies are not ultimate. The works dedicated to the particle size control and carbon coating considered, in

* Corresponding author. Tel.: +49 2518336083; fax: +49 2518336084.
E-mail address: andrea.balducci@uni-muenster.de (A. Balducci).

0378-7753/$ – see front matter © 2012 Elsevier B.V. All rights reserved.
http://dx.doi.org/10.1016/j.jpowsour.2012.11.125

most of the cases, electrodes with composition not suitable for real application [13,14]. In the case of the use of a fraction of the total capacity, it is not possible to obtain capacities significantly higher with respect to the state-of-the-art graphite. Taking into account this situation, it is clear that the realization of α-Fe_2O_3 nano-particles easily usable for the preparation of composite electrodes and, at the same time, able to guarantee the full capacity of this anodic material could be extremely important for the development of advanced and safer LIBs.

Herein we propose the use of ferrocene as a precursor for the synthesis of carbon-coated α-Fe_2O_3 nano-particles [20]. The pyrolysis of ferrocene leads to the formation of a compound that, if is properly oxidized, can be fully converted into carbon-coated α-Fe_2O_3 nano-particles. This simple, fast and cheap synthetic route consent the realization of carbon-coated nano-particles with very homogenous shape and particle size. Moreover, it also allows a precise control of the carbon coating present on the nano-particles. The carbon-coated α-Fe_2O_3 nano-particles obtained using this synthetic route can be easily and safely processed in water to realize composite electrodes with a composition suitable for practical application. When used in combination with conventional electrolytes such electrodes display high specific capacity, excellent cycling retention, and remarkable rate performance.

2. Experimental

Carbon-coated α-Fe_2O_3 was synthesized by pyrolysis of ferrocene (Merck, ferrocene for synthesis) followed by an oxidation in oxygen/nitrogen gas atmosphere. The pyrolysis of ferrocene was performed in a quartz tube reactor inside a horizontal furnace (P330, Nabertherm). A known amount of ferrocene powder was sublimated (200–300 °C) under argon atmosphere in the heating zone of the furnace. The ferrocene vapor was carried by a constant Ar flow into the furnace, where the pyrolysis occurred at 1050 °C. The oxidation of the ferrocene pyrolysis products was carried out under a constant artificial air flow at elevated temperatures in the same quartz tube reactor inside a horizontal furnace. A constant O_2/N_2 (20:80) gas mixture flow (equal to 114 mL min^{-1} O_2 and 455 mL min^{-1} N_2, respectively) was applied. The samples were heated (5 °C min^{-1}) from room temperature to the target temperature (ranging from 430 to 700 °C), which was than kept for 2 h before cooling down to room temperature.

The morphology and crystal structure of the materials were identified by high resolution scanning electron microscopy (HRSEM), high resolution energy-filtering transmission electron microscopy (EFTEM), powder X-ray diffraction (XRD) and Raman spectroscopy. HRSEM measurements were carried out using a ZEISS Auriga® microscope and EFTEM measurements were performed on a ZEISS LIBRA® 200 FE device, while the XRD measurements were carried out using a Bruker D8 Advance (Cu-Kα-radiation, $\lambda = 0.154$ nm). Raman spectroscopy was performed using a SENTERRA Raman spectrometer (BRUKER Optics), equipped with a 532 nm laser and an output power of 2 mW. The carbon content of the nano-particles was estimated using CHN-elemental analysis (CHN-O-Rapid, Heraeus). The specific BET surface area of the carbon-coated iron oxide particles was measured using the ASAP 2020 from Micromeritics Instrument Corporation (USA).

Electrodes containing carbon-coated α-Fe_2O_3 nano-particles were prepared using a fabrication process similar to that reported in Ref. [27]. The composition of the dried electrode was of 85% active material, 10 wt.% conducting carbon (Super C65, Timcal) and 5 wt.% sodium carboxymethyl-cellulose (CMC, Walocel CRT 2000 PPA 12 from Dow Wolff Cellulosics). The electrode active material mass loading was ca. 1.5 mg cm^{-2}; the electrode area was 1.13 cm^2. The electrochemical investigations were carried out using Swagelok® cells. Metallic lithium foils or oversized cathodes containing lithium iron phosphate (LFP, Süd-Chemie) were used as the counter electrodes, while metallic lithium foil was utilized as the reference electrode. A solution of 1 M $LiPF_6$ (Sigma–Aldrich) in propylene carbonate (PC, UBE, Japan) was used as electrolyte. In all experiments a Whatman GF/D glass microfiber filter (thickness: 675 μm) with a diameter of 12 mm was used as separator and drenched with 100 μL of the used electrolyte.

Cyclic voltammetries (CV) were performed on a VMP multichannel potentiostatic–galvanostatic system (Biologic Science Instrument, France), whereas galvanostatic cycling (CC) was carried out using a Maccor series 4300 battery tester. All potentials reported in this work refer to the Li/Li^+ couple.

3. Results and discussion

3.1. Preparation and characterization of carbon-coated α-iron oxide

The pyrolysis of ferrocene at 1050 °C leads to a compound containing a mixture of different nanostructures made out of carbon and iron (Fig. 1a) [21]. This process yields mainly a black powder with some flat and pure glittering iron particles. The products are elemental iron (32 wt. %) and carbon (68 wt.%). The yield is very high (>95%) since only low amounts of carbon and/or iron particles fumed off. The XRD diffraction pattern of this compound (Fig. 1b) shows a peak at about 26.2°, which can be assigned to the (002) plane of hexagonal graphitic structure, with

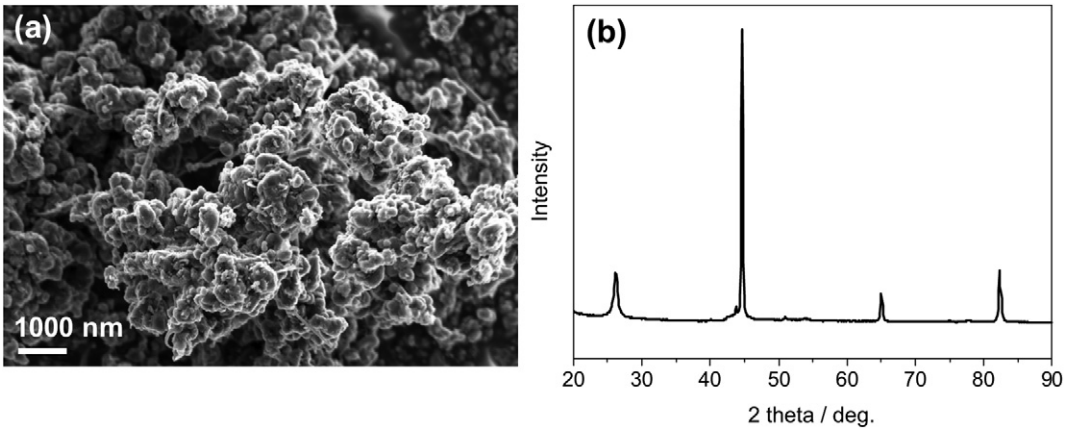

Fig. 1. SEM image (a) and XRD pattern (b) of the compounds obtained by pyrolysis of ferrocene.

an interlayer spacing of 0.34 nm. This peak is symmetric and narrow, indicating a high crystallinity of the sample. The peaks at 44.8°, 65.1° and 82.5° can be identified as the (110), (200) and (211) planes of body-centered cubic (bcc) lattice of iron α-phase, respectively. Their intensities and positions quantitatively confirm that α-Fe phase dominates in all samples.

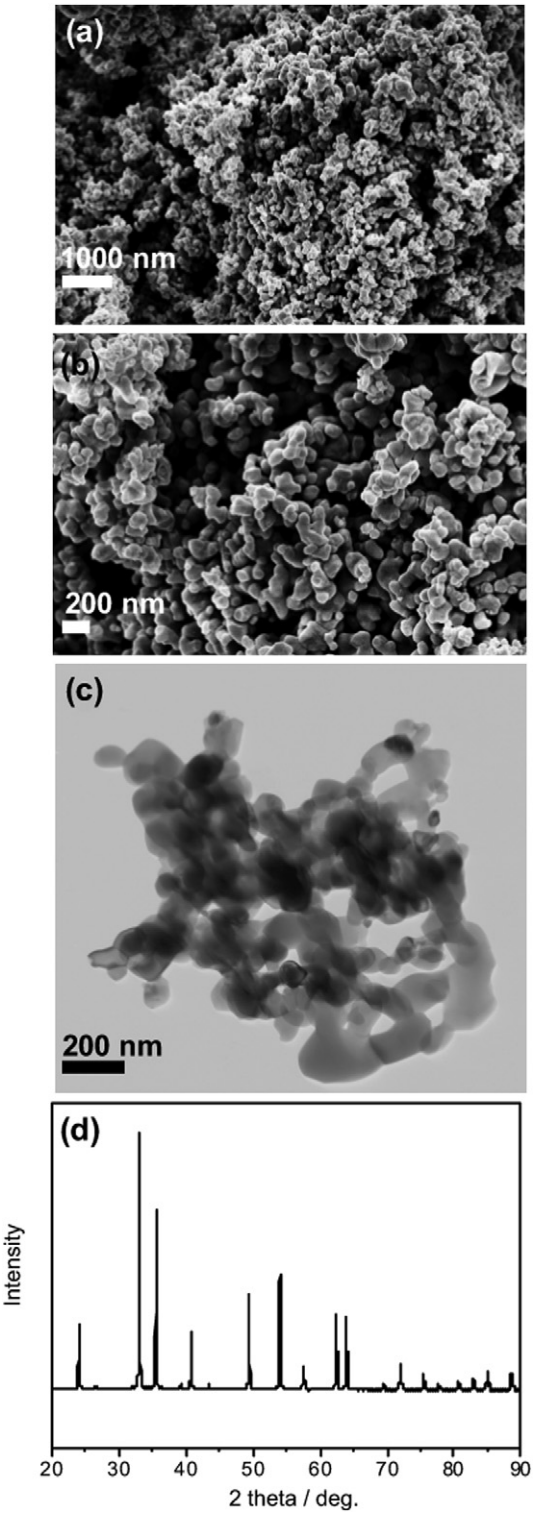

Fig. 2. SEM images (a, b), TEM image (c) and XRD pattern (d) of the carbon-coated α-Fe_2O_3 nano-particles obtained using an oxidation temperature of 700 °C.

Table 1
Crystal size along different crystallographic directions for α-Fe_2O_3 powder.

$D_{(1\,0\,4)}$ (nm)	$D_{(1\,1\,0)}$ (nm)	$D_{(0\,2\,4)}$ (nm)	$D_{(1\,1\,6)}$ (nm)	$D_{(2\,1\,4)}$ (nm)	$D_{(3\,0\,0)}$ (nm)	$D_{(0\,1\,2)}$ (nm)
82.03	82.58	87.42	86.55	86.76	86.70	77.34

When this mixture of different nanostructures is oxidized at 430–700 °C the carbon shells formed during the pyrolysis process gets thinner, and the iron core can be oxidized. As a result, the compounds are completely converted into carbon-coated α-Fe_2O_3 nano-particles (e.g. the oxidation of 3 g of pyrolysis products obtained at 700 °C leads to the formation of about 1.4 g carbon-coated iron oxide, corresponding to a yield >99%). As shown in the SEM images, the oxidation process leads to the formation of nano-particles with very homogenous shape and particle size (Fig. 2a and b). From the TEM image the primary particle size can be estimated between 50 and 150 nm, and it can be seen that the particles tend to agglomerate in chain-like structures (Fig. 2c). The high purity and crystallinity could be confirmed by the XRD pattern of carbon-coated iron oxide powder. The pattern is in good agreement to that of the hexagonal α-Fe_2O_3 phase, and the sharp peaks observed in the pattern indicate the high crystallinity of the formed nano-particles [22]. The similar intensities of the diffraction peaks at 33.2° and 35.7° indicate a spherical shape for the crystals in the sample, and using Scherrer's equation [23,24] an average particle size of 80–90 nm could be roughly estimated (see Table 1). As indicated in Table 2, the carbon-coated α-Fe_2O_3 nano-particles (oxidized at 700 °C), display BET surface area of 2.9 $m^2\,g^{-1}$, with negligible micro- and meso-porosity. Table 3 indicates the influence of the oxidation temperature on the carbon content of the α-Fe_2O_3 nano-particles. As shown, when an oxidation temperature of 430 °C is used, the α-Fe_2O_3 nano-particles display a carbon content of 10.11%. If the oxidation temperature is increased to 700 °C, the carbon content of the nano-particles decreases to 0.04%. This difference clearly shows that the carbon coating can be easily controlled varying the oxidation temperature. In order to acquire additional information about the carbon coating of the α-Fe_2O_3 nano-particles, Raman spectroscopy was used. With the aim to investigate also the uniformity of the coating, different parts of the considered samples were investigated. The Raman spectra of the samples with different carbon content are shown in Fig. 3. Three main bands were considered: the D-band at ~1350 cm^{-1}, which represents the defects in the carbon structure, the 2D-band at ~2690 cm^{-1}, which can be used to determine the graphene layer thickness, and the G-band at ~1580 cm^{-1}, which is the main band in graphite and graphene representing the planar sp^2 bonded structure. As shown, the typical modes for α-Fe_2O_3 can be observed in the so-called "finger print" region at low wave numbers. Unfortunately, the D-band is overlain by an iron oxide vibration as can be seen in Fig. 3. However, the G-band is present and its intensity decreases, as expected, with decreasing carbon content in the iron oxide samples. Even at oxidation temperatures above 600 °C some small intense G-band vibrations could be observed, indicating that still some carbon is present. Also the 2D-band could be observed and, as shown in the figure, its intensity decreases with the decrease of carbon content in the samples. Considering these results, a homogenous carbon coating seems to be present on the surface of the iron oxide

Table 2
Estimated average particle size and specific BET surface area for α-Fe_2O_3 powder.

Average particle size TEM/nm	Average particle size XRD/nm	Specific BET surface area/$m^2\,g^{-1}$
50–100	84	2.9

Table 3
Carbon content obtained by CHN-analysis for α-Fe_2O_3 powder oxidized at different temperatures.

Material	Carbon content / wt.%
Fe_2O_3 430 °C	10.11
Fe_2O_3 470 °C	7.45
Fe_2O_3 500 °C	3.21
Fe_2O_3 600 °C	0.05
Fe_2O_3 700 °C	0.04

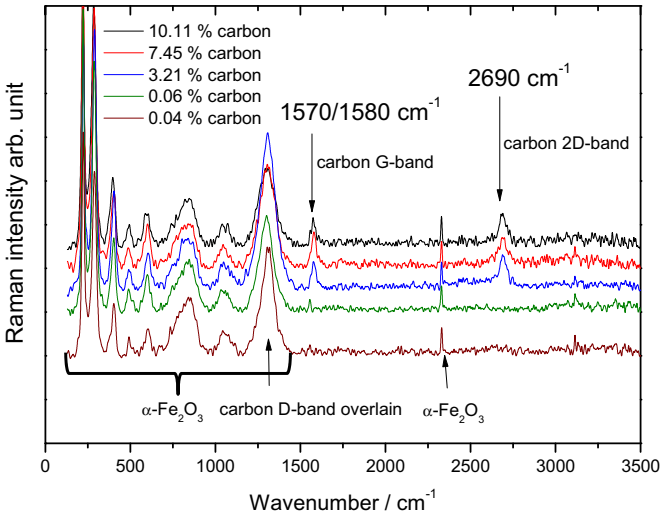

Fig. 3. Raman spectra of the carbon-coated α-Fe_2O_3 nano-particles with different carbon content obtained after oxidation at temperatures between 430 and 700 °C.

particles. The carbon coating appears to consist of mainly amorphous carbon with a minor graphitic fraction. In order to investigate the thickness of the coating, EDX measurements were carried out at different parts of the sample obtained using an oxidation temperature of 700 °C. These measurements (not shown) indicated that the surface of the iron oxide particles is covered by a carbon layer with a thickness of ca. 4–10 nm. Taking into account these results, the α-Fe_2O_3 nano-particles seem therefore to display a rather uniform coating, distributed over their entire surface. Nevertheless, further investigations should be beneficial to characterize more in detail the characteristics of the coating of the nano-particles.

It is important to note that in abovementioned synthesis no solvents or cleaning steps are required to obtain very homogeneous carbon-coated α-Fe_2O_3 nano-particles. Moreover, the coating on the particles can be easily controlled during the oxidation step, and no further coating processes are necessary after the synthesis.

3.2. Electrochemical characterization of carbon-coated α-Fe_2O_3 electrodes

Composite electrodes containing the carbon-coated α-Fe_2O_3 nano-particles were prepared using aqueous slurries and their electrochemical performance was investigated by cyclic voltammetry (CV) and galvanostatic charge/discharge cycling (CC), using 1M $LiPF_6$ in propylene carbonate (PC) as electrolyte. Fig. 4 shows the CV profiles of the investigated electrodes in two different potential ranges: from 3.0 V to 0.6 V vs. Li/Li^+ (Fig. 4a), and from 3.0 V to 0.08 V vs. Li/Li^+ (Fig. 4b). In the case of the first potential range, the electrode was coated over an Al current collector, while in the case of the second potential range a Cu current collector was used. As shown in the figures, the full reduction of Fe_2O_3 into elemental iron and amorphous lithia (Li_2O) occurred at a potential of 0.8 V vs. Li/Li^+ in both electrodes, as indicated by the first, large cathodic peak visible in the CV [7]. During the first de-lithiation process, where the oxidation reaction of Fe^0 to Fe^{3+} took place [15], an anodic peak at 1.60 vs. Li/Li^+ and a "shoulder" at 1.76 V vs. Li/Li^+ were recorded. Starting from the second cycle, both cathodic and anodic peaks shifted towards positive potential. The intensity of both peaks slightly changed during the first cycles, but starting from the fourth cycle became constant. The coulombic efficiency of the first lithiation-de-lithiation process was of 72%, and the resulting capacity loss was 28%. This loss of capacity is often attributed to the decomposition of electrolyte to form a SEI layer [4,7,25]. Nevertheless, it is interesting to note that no evident electrolyte decomposition processes were observed in the investigated electrodes, and that the efficiency of the process was close to 99% already from the second cycle. This high efficiency could be related to the electrochemical stability of PC, as well as to the morphology and purity of the α-Fe_2O_3 nano-particles [26]. However, more investigations are needed to clarify this point.

During the first lithiation process of the CC tests, the electrodes displayed specific capacities of about 1000 mAh g^{-1} in the potential range between 3.0 V and 0.6 V vs. Li/Li^+ (Al current collector, Fig 5a), and 1150 mAh g^{-1} between 3.0 V and 0.08 V vs. Li/Li^+ (Cu current collector, Fig. 5b). Both electrodes displayed a plateau at

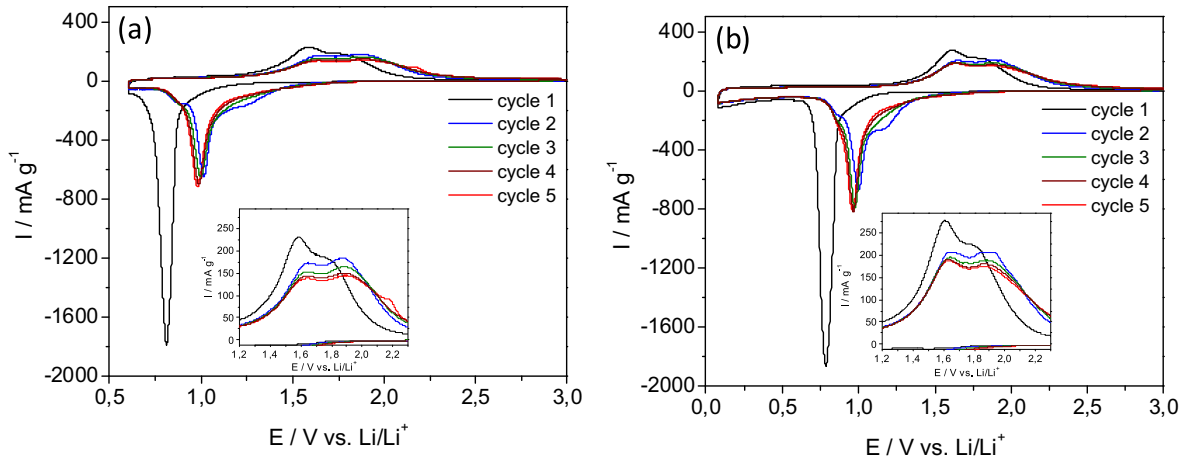

Fig. 4. Cyclic voltammetry of carbon-coated α-Fe_2O_3 based electrodes cycled between 3.0 V and 0.6 V vs. Li/Li^+ (a) and between 3.0 V and 0.08 V vs. Li/Li^+ (b) using a scan rate of 50 μV s^{-1}. The nano-particles were obtained using an oxidation temperature of 700 °C.

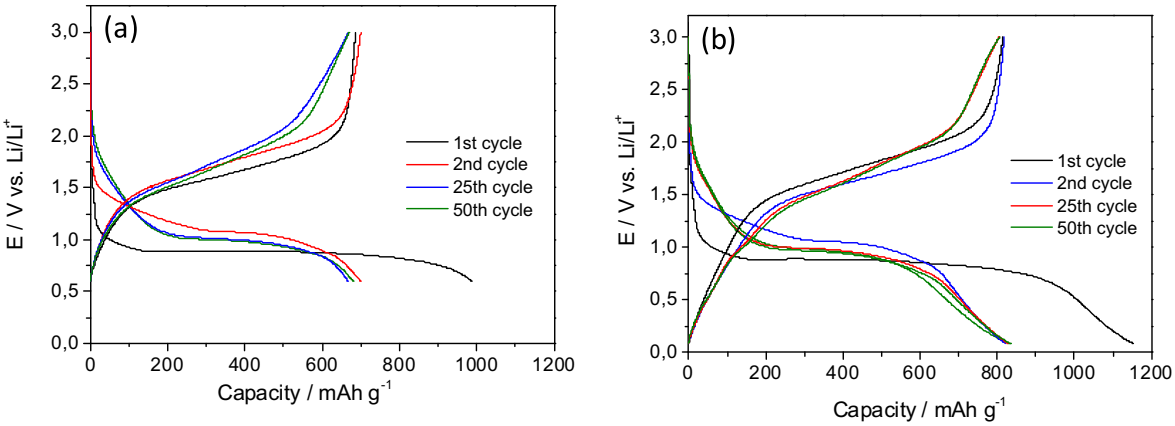

Fig. 5. Voltage profiles of carbon-coated α-Fe_2O_3 based electrodes cycled between 3.0 V and 0.6 V vs. Li/Li^+ (a) and between 3.0 V and 0.08 V vs. Li/Li^+ (b) using a current density corresponding to C/8. The nano-particles were obtained using an oxidation temperature of 700 °C.

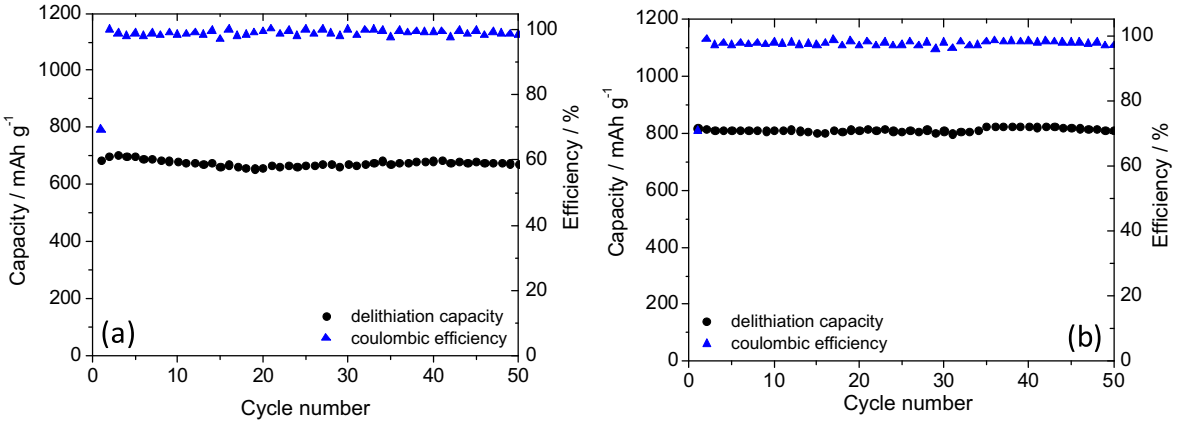

Fig. 6. Discharge capacity and coulombic efficiency of carbon-coated α-Fe_2O_3 based electrodes cycled between 3.0 V and 0.6 V vs. Li/Li^+ (a) and between 3.0 V and 0.08 V vs. Li/Li^+ (b) using a current density corresponding to C/8. The nano-particles were obtained using an oxidation temperature of 700 °C.

0.9 V vs. Li/Li^+. During the first de-lithiation process the electrodes delivered a capacity of about 700 mAh g^{-1} and 850 mAh g^{-1} in the potential range between 3.0 V and 0.6 V vs. Li/Li^+ and 3.0 V and 0.08 V vs. Li/Li^+, respectively. As shown in the figure, the profiles of charge–discharge were rather different during the first cycles, but become similar during the cycling. This behavior is typical for MO-based electrodes and it is attributed to the conversion process [25]. Starting from the second cycle the efficiency of the charge–discharge process was always close to 99%, and the electrodes displayed specific capacity of 700 mAh g^{-1} between 3.0 V and 0.6 V vs. Li/Li^+ (Al current collector, Fig 5a), and 820 mAh g^{-1} between 3.0 V and 0.08 V vs. Li/Li^+ (Cu current collector, Fig. 5b). As shown in Fig. 6, these high capacities were fully maintained for 50 cycles (capacity retention higher than 99%) in both potential ranges. When current densities of 5.04 A g^{-1} were applied during the charge–discharge process, the electrodes delivered capacities of 330 mAh g^{-1} between 3.0 V and 0.6 V vs. Li/Li^+ and 420 mAh g^{-1} between 3.0 V and 0.6 V vs. Li/Li^+. To the best of our knowledge, this performance, especially in terms of capacity retention and coulombic efficiency, is among the highest so far reported for α-Fe_2O_3 based electrodes.

As mentioned above, when the considered synthetic route is used, the carbon content of the α-Fe_2O_3 nano-particles can be controlled varying the oxidation temperature. Fig. 7 compares the capacity retention of an electrode containing 10% of carbon with that of the electrode coated on Al current collector considered

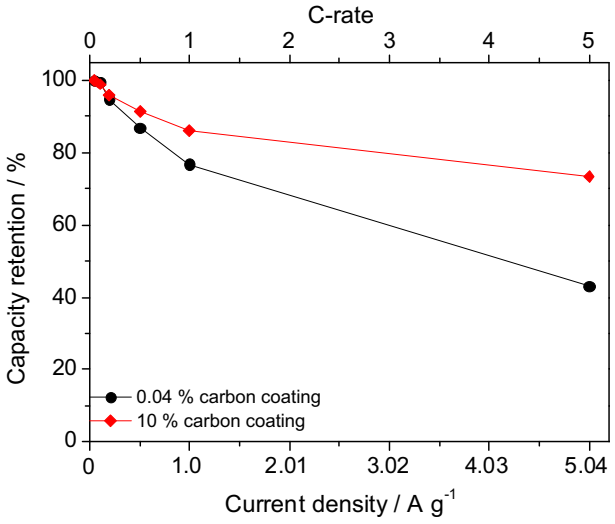

Fig. 7. Capacity retention of carbon-coated α-Fe_2O_3 based electrodes with different carbon content during tests carried out between 3.0 V and 0.6 V vs. Li/Li^+, utilizing current densities ranging from 0.3 A g^{-1} to 5.04 A g^{-1}.

above, with a carbon content of 0.04%. Both electrodes were cycled between 3.0 V and 0.6 V vs. Li/Li^+ using current densities ranging from 0.3 A g^{-1} to 5.04 A g^{-1}. As shown in the figure, the composite electrode containing 10% carbon showed capacity retention of almost 80% during cycling carried out at 5.04 A g^{-1}. Taking into account this impressive capacity retention, the carbon-coated α-Fe_2O_3 nano-particles appear as promising candidate also for the realization of lithium-ion capacitors and/or high power batteries.

4. Conclusion

In this work we showed that ferrocene can be conveniently used as precursor for the synthesis of carbon-coated α-Fe_2O_3 nano-particles with homogeneous nano-structure, high crystallinity and high purity. These nano-particles can be easily used for the realization of composite electrodes with composition suitable for practical application. Composite electrodes made of carbon-coated α-Fe_2O_3 nano-particles display outstanding performance in terms of specific capacity and cycling stability. Moreover, depending on their carbon content, they might display very high capacity retention at high current density. These characteristics make these electrodes attractive for several electrochemical devices, including high power systems. Finally, it is important to note that the simple, fast and cheap synthetic route here presented can be easily implemented also for other metallocenes [20] (e.g. cobaltocene, etc.) and, therefore, can be considered as a new strategy for the realization of carbon-coated MO nano-particles for energy storage devices.

Acknowledgments

The authors wish to thank the university of Münster, the Ministry of Innovation, Science and Research of North Rhine-Westphalia (MIWF) within the project “Superkondensator und Lithium-Ionen-Hybrid-Superkondensatoren auf der Basis ionischer Flüssigkeiten” for the financial support.

References

[1] A.S. Arico, P. Bruce, B. Scrosati, J.-M. Tarascon, W. van Schalkwijk, Nature Materials 4 (2005) 366.
[2] J. Maier, Nat Mater 4 (2005) 805.
[3] D. Bresser, E. Paillard, E. Binetti, S. Krueger, M. Striccoli, M. Winter, S. Passerini, Journal of Power Sources.
[4] M.F. Hassan, M.M. Rahman, Z.P. Guo, Z.X. Chen, H.K. Liu, Electrochimica Acta 55 (2010) 5006.
[5] P.G. Bruce, B. Scrosati, J.-M. Tarascon, Angewandte Chemie 120 (2008) 2972.
[6] P. Poizot, S. Laruelle, S. Grugeon, L. Dupont, J.M. Tarascon, Nature 407 (2000) 496.
[7] D. Larcher, D. Bonnin, R. Cortes, I. Rivals, L. Personnaz, J.M. Tarascon, Journal of the Electrochemical Society 150 (2003) A1643.
[8] M.M. Thackeray, W.I.F. David, J.B. Goodenough, Journal of Solid State Chemistry 55 (1984) 280.
[9] S. Morzilli, B. Scrosati, Electrochimica Acta 30 (1985) 1271.
[10] K.M. Abraham, D.M. Pasquariello, E.B. Willstaedt, Journal of the Electrochemical Society 137 (1990) 743.
[11] J. Hassoun, F. Croce, I. Hong, B. Scrosati, Electrochemistry Communications 13 (2011) 228.
[12] E. García-Tamayo, M. Valvo, U. Lafont, C. Locati, D. Munao, E.M. Kelder, Journal of Power Sources 196 (2011) 6425.
[13] H. Liu, D. Wexler, G. Wang, Journal of Alloys and Compounds 487 (2009) L24.
[14] P.C. Wang, H.P. Ding, T. Bark, C.H. Chen, Electrochimica Acta 52 (2007) 6650.
[15] Y. NuLi, P. Zhang, Z. Guo, P. Munroe, H. Liu, Electrochimica Acta 53 (2008) 4213.
[16] H. Suk Ryu, J. Seon Kim, Z. Guo, H. Liu, K. Won Kim, J. Hyeon Ahn, H. Jun Ahn, vol. T139, 2010.
[17] H. Morimoto, S.-i. Tobishima, Y. Iizuka, Journal of Power Sources 146 (2005) 315.
[18] H. Liu, G. Wang, J. Wang, D. Wexler, Electrochemistry Communications 10 (2008) 1879.
[19] D. Larcher, C. Masquelier, D. Bonnin, Y. Chabre, V. Masson, J.B. Leriche, J.M. Tarascon, Journal of the Electrochemical Society 150 (2003) A133.
[20] Deutsches Patentamt, Aktenzeichen DE 10 2012 100 789.
[21] Q. Liu, Z.-G. Chen, B. Liu, W. Ren, F. Li, H. Cong, H.-M. Cheng, Carbon 46 (2008) 1892.
[22] M. Sorescu, L. Diamandescu, D. Tarabasanu-Mihaila, V.S. Teodorescu, B.H. Howard, Journal of Physics and Chemistry of Solids 65 (2004) 1021.
[23] P. Scherrer, Göttinger Nachrichten Mathematics and Physics 2 (1918) 98.
[24] U. Holzwarth, N. Gibson, Nature Nanotechnology 6 (2011) 534.
[25] J.-M. Tarascon, S. Grugeon, M. Morcrette, S. Laruelle, P. Rozier, P. Poizot, Comptes Rendus Chimie 8 (2005) 9.
[26] M.R. Palacin, D. Larcher, A. Audemer, N. Sac-Epee, G.G. Amatucci, J.M. Tarascon, Journal of the Electrochemical Society 144 (1997) 4226.
[27] A. Krause, P. Kossyrev, M. Oljaca, S. Passerini, M. Winter, A. Balducci, Journal of Power Sources 196 (2011) 8836.